

Nonlinear longitudinal current of band-geometric origin in wires of finite thickness

Robin Durand,¹ Louis-Thomas Gendron,¹ Théo Nathaniel Dionne,¹ and Ion Garate¹

¹*Département de physique, Institut quantique and Regroupement Québécois sur les Matériaux de Pointe, Université de Sherbrooke, Sherbrooke, Québec J1K 2R1, Canada*

(Dated: February 23, 2024)

The miniaturization of integrated circuits is facing an obstruction due to the escalating electrical resistivity of conventional copper interconnects. The underlying reason for this problem was unveiled by Fuchs and Sondheimer, who showed that thinner wires are more resistive because current-carrying electrons encounter the rough surfaces of the wire more frequently therein. Here, we present a generalization of the Fuchs-Sondheimer theory to Dirac and Weyl materials, which are candidates for next-generation interconnects. We predict a nonlinear longitudinal electric current originating from the combined action of the Berry curvature and non-specular surface-scattering.

Introduction.— A strong research effort is currently underway to find new interconnect materials that will replace copper in integrated circuits [1, 2]. Topological materials, endowed with their robust and highly conducting surface states, have the potential [3–7] to overturn the unfavorable resistivity scaling predicted by Fuchs [8] and Sondheimer [9] for conventional wires.

In this work, we generalize the Fuchs-Sondheimer (FS) theory to materials with nonzero electronic Berry curvature. For a homogeneous wire with time-reversal symmetry, we predict an electric current of band-geometric origin along the wire axis, which is quadratic in the applied electric field. While nonlinear Hall effects produced by the Berry curvature [10, 11] have been observed [12, 13], the nonlinear longitudinal current found below is fundamentally different. It emerges from the combined action of the Berry curvature and the non-specular scattering at the wire boundaries. Earlier studies [14–17] of nonlinear currents associated to the quantum metric tensor have ignored wire boundaries, therefore overlooking the effect we predict.

Methodology.— We consider conducting materials with low-energy electronic valleys. The electronic energy dispersion in the vicinity of valley χ is denoted as $\varepsilon_{\mathbf{p}}^{\chi}$, where \mathbf{p} is the momentum measured from the valley center. The system is finite in the z direction, $z \in [-a/2, a/2]$, but infinite in the remaining directions. By assuming that there is only one band that intersects the Fermi energy, we are (i) neglecting size quantization effects (i.e. a must be much larger than the Fermi wavelength), and (ii) omitting the potential presence of topological surface states (we focus on the transport properties of bulk electrons).

The semiclassical transport under a uniform and constant electric field, $\mathbf{E} = E_x \hat{\mathbf{x}}$, is described by the steady-state Boltzmann equation

$$\dot{\mathbf{r}}_{\mathbf{p}}^{\chi} \cdot \nabla_{\mathbf{r}} f_{\mathbf{p}}^{\chi}(\mathbf{r}) + \dot{\mathbf{p}} \cdot \nabla_{\mathbf{p}} f_{\mathbf{p}}^{\chi}(\mathbf{r}) = \mathcal{I}_{\mathbf{p}}^{\chi}, \quad (1)$$

where $f_{\mathbf{p}}^{\chi}(\mathbf{r})$ is the electronic occupation,

$$\begin{aligned} \dot{\mathbf{r}}_{\mathbf{p}}^{\chi} &= \mathbf{v}_{\mathbf{p}}^{\chi} + \dot{\mathbf{p}} \times \boldsymbol{\Omega}_{\mathbf{p}}^{\chi} / \hbar \\ \dot{\mathbf{p}} &= -e\mathbf{E} \end{aligned} \quad (2)$$

are the electronic group velocity and force, $\mathbf{v}_{\mathbf{p}}^{\chi} = \nabla_{\mathbf{p}} \varepsilon_{\mathbf{p}}^{\chi}$, $\boldsymbol{\Omega}_{\mathbf{p}}^{\chi}$ is the Berry curvature in valley χ and

$$\mathcal{I}_{\mathbf{p}}^{\chi} = -\frac{1}{\rho(\varepsilon_{\mathbf{p}}^{\chi})\tau} \sum_{\mathbf{p}'} \delta(\varepsilon_{\mathbf{p}}^{\chi} - \varepsilon_{\mathbf{p}'}^{\chi}) (f_{\mathbf{p}}^{\chi} - f_{\mathbf{p}'}^{\chi}) \quad (3)$$

is the collision integral describing elastic scattering with bulk impurities in the lowest Born approximation. Here, τ is the mean scattering time and $\rho(\varepsilon)$ is the density of states at energy ε . Treating the valleys independently is justified if the intravalley scattering time is much shorter than the intervalley scattering time, which we assume to be the case for the sake of simplicity. Likewise, we neglect skew-scattering and side-jump processes.

We solve Eq. (1) perturbatively in powers of E_x up to second order, $f_{\mathbf{p}}^{\chi} \simeq f_{0,\mathbf{p}}^{\chi} + f_{1,\mathbf{p}}^{\chi} + f_{2,\mathbf{p}}^{\chi}$, where $f_{n,\mathbf{p}}^{\chi} \propto E_x^n$. For $n \geq 1$, we apply the boundary condition of Fuchs and Sondheimer [8, 9]: $f_{n,\mathbf{p}}^{\chi}(x, y, -a/2) = 0$ if $v_{\mathbf{p},z}^{\chi} > 0$, and $f_{n,\mathbf{p}}^{\chi}(x, y, a/2) = 0$ if $v_{\mathbf{p},z}^{\chi} < 0$. Physically, the electron distribution on each valley is in equilibrium immediately after a collision with the wire boundary. In the boundary conditions, $v_{\mathbf{p},z}^{\chi}$ appears instead of $\dot{z}_{\mathbf{p}}^{\chi}$; this is a consequence of solving Eq. (1) perturbatively in E_x .

The longitudinal electric current density reads

$$j_x(\mathbf{r}) = \sum_{\chi} j_x^{\chi}(\mathbf{r}) = -e \sum_{\chi} \int \frac{d^d p}{(2\pi\hbar)^d} \dot{x}_{\mathbf{p}}^{\chi} f_{\mathbf{p}}^{\chi}(\mathbf{r}), \quad (4)$$

where d is the dimensionality of the system and j_x^{χ} is the valley-resolved current density along x . Note that Eq. (4) does not include the contribution from the orbital magnetic moment of electrons to the transport current [18]. This omission does not change the main prediction of our paper.

Broken translational symmetry along z implies $f_{\mathbf{p}}^{\chi}(\mathbf{r}) = f_{\mathbf{p}}^{\chi}(z)$ and $j_x(\mathbf{r}) = j_x(z)$. We write

$$j_x(z) \simeq \sum_{\chi} [j_{1,x}^{\chi}(z) + j_{2,x}^{\chi}(z)] = j_{1,x}(z) + j_{2,x}(z), \quad (5)$$

where $j_{n,x}(z) \propto E_x^n$. The effective linear ($\bar{\sigma}_1$) and nonlinear ($\bar{\sigma}_2$) conductivities are obtained by averaging the current density over the wire thickness,

$$\bar{j}_x = \frac{1}{a} \int_{-a/2}^{a/2} dz j_x(z) \simeq \bar{\sigma}_1 E_x + \bar{\sigma}_2 E_x^2. \quad (6)$$

Solution of Eq. (1).– At zeroth order in E_x , Eq. (1) yields $f_{\mathbf{p}}^x = f_{0,\mathbf{p}}^x$ and $\partial_z f_{0,\mathbf{p}}(z) = 0$. Using this, the Boltzmann equation at first order in E_x reads

$$v_{\mathbf{p},z}^x \frac{\partial f_{1,\mathbf{p}}^x}{\partial z} - eE_x \frac{\partial f_{0,\mathbf{p}}^x}{\partial p_x} = \mathcal{I}_{1,\mathbf{p}}^x, \quad (7)$$

where $\mathcal{I}_{1,\mathbf{p}}^x$ is given by Eq. (3) with $f \rightarrow f_1$. The second term on the left hand side acts as a source term that forces $f_{1,\mathbf{p}}^x \neq 0$. Assuming that $\varepsilon_{\mathbf{p}}^x$ is invariant under $p_x \rightarrow -p_x$ (this assumption enables us to treat $\mathcal{I}_{1,\mathbf{p}}^x$ beyond the relaxation time approximation (RTA) [19]), the source term is odd in p_x . Therefore, if we decompose f_1 in a part that is even in p_x and a part that is odd, only the latter is nonzero according to Eq. (7). Further imposing the FS boundary conditions, we reach

$$f_{1,\mathbf{p}}^x = \begin{cases} h_{1,\mathbf{p}}^x \left(1 - e^{-(z+a/2)/v_{\mathbf{p},z}^x \tau} \right), & v_{\mathbf{p},z}^x > 0 \\ h_{1,\mathbf{p}}^x \left(1 - e^{-(z-a/2)/v_{\mathbf{p},z}^x \tau} \right), & v_{\mathbf{p},z}^x < 0 \end{cases}, \quad (8)$$

where

$$h_{1,\mathbf{p}}^x \equiv eE_x \tau \frac{\partial f_{0,\mathbf{p}}^x}{\partial p_x}. \quad (9)$$

The electronic occupation becomes z -dependent at linear order in E_x . This position-dependence is significant only in the proximity to $z = a/2$ (for $v_{\mathbf{p},z}^x < 0$) and $z = -a/2$ (for $v_{\mathbf{p},z}^x > 0$). Far enough from the wire surfaces, Eq. (8) converges to the standard expression for infinite systems, $h_{1,\mathbf{p}}^x$, independent of z . These results are identical to the ones obtained by Fuchs and Sondheimer [8, 9], i.e. unaffected by the Berry curvature of electrons.

New results arise at second order in E_x , where the Boltzmann equation reads [19]

$$v_{\mathbf{p},z}^x \frac{\partial f_{2,\mathbf{p}}^x}{\partial z} + \frac{eE_x \Omega_{\mathbf{p},y}^x}{\hbar} \frac{\partial f_{1,\mathbf{p}}^x}{\partial z} - eE_x \frac{\partial f_{1,\mathbf{p}}^x}{\partial p_x} = \mathcal{I}_{2,\mathbf{p}}^x. \quad (10)$$

Here, the y -component of the Berry curvature appears in a source term for f_2 . Now, the two source terms (involving $\partial_z f_1^x$ and $\partial_{p_x} f_1^x$, respectively) do not in general have the same parity under $p_x \rightarrow -p_x$. Therefore, if we decompose f_2 in a part that is even in p_x and a part that is odd (once again under the assumption of $\varepsilon_{\mathbf{p}}^x$ being an even function of p_x), both parts are nonzero according to Eq. (7). The collision term for the even part cannot be solved analytically without invoking approximations such as RTA, which we wish to avoid in order to respect conservation laws. Fortunately, for the electric current in Eq. (4), only the part of f_2 that is odd in p_x matters [20]. This part can be analytically obtained without resorting to RTA:

$$f_{2,\mathbf{p}}^x \ni \begin{cases} h_{2,\mathbf{p}}^x(z+a/2) e^{-(z+a/2)/v_{\mathbf{p},z}^x \tau}, & v_{\mathbf{p},z}^x > 0 \\ h_{2,\mathbf{p}}^x(z-a/2) e^{-(z-a/2)/v_{\mathbf{p},z}^x \tau}, & v_{\mathbf{p},z}^x < 0, \end{cases} \quad (11)$$

where

$$h_{2,\mathbf{p}}^x \equiv \frac{e^2 E_x^2 \Omega_{\mathbf{p},y}^x}{\hbar (v_{\mathbf{p},z}^x)^2} \frac{\partial f_{0,\mathbf{p}}^x}{\partial p_x}. \quad (12)$$

Interestingly, Eq. (11) is proportional to the y -component of the Berry curvature and emerges because $f_{1,\mathbf{p}}^x$ is z -dependent. Unlike $f_{1,\mathbf{p}}^x$, $f_{2,\mathbf{p}}^x$ is negligible far enough from the wire edges. In our theory, the absence of an $O(E_x^2)$ current far from the edges is a consequence of the assumed invariance of $\varepsilon_{\mathbf{p}}^x$ under $p_x \rightarrow -p_x$. When this assumption is relaxed, we find that there can be an additional $O(E_x^2)$ current density independent of Berry curvature for all z , provided that the crystal lacks time-reversal symmetry [21]. More so, should we incorporate skew-scattering processes in our theory, an $O(E_x^2)$ current density could likewise emerge for all z even if $\varepsilon_{\mathbf{p}}^x$ were invariant under $p_x \rightarrow -p_x$, and even in non-magnetic crystals [22].

Equation (11) foreshadows a nonlinear, surface-localized longitudinal current that originates from the joint presence of nontrivial band geometry and diffusive scattering at the wire's surfaces. The precise form of that current is system-dependent. To make further progress, we next focus on Dirac and Weyl materials.

Two dimensional Dirac metal.– We consider two valleys of massive Dirac fermions in the xz plane, with $x \in (-\infty, \infty)$ and $z \in [-a/2, a/2]$. We suppose that the Fermi energy ε_F intersects the conduction band, whose dispersion at valley χ ($\chi = \pm 1$) is approximated as

$$\varepsilon_{\mathbf{p}}^x = \sqrt{c^2 p^2 + m^2} + \alpha_z^x p_z, \quad (13)$$

Here, c is the Fermi velocity, $\mathbf{p} = (p_x, p_z)$ is the momentum measured from the band edge, m is the Dirac mass and α_z^x is the tilt velocity along the p_z direction. The Berry curvature of the conduction band reads [23]

$$\Omega_{\mathbf{p}}^x = \chi \frac{m \hbar^2 c^2}{2(c^2 p^2 + m^2)^{3/2}} \hat{\mathbf{y}}. \quad (14)$$

We adopt a model in which the two valleys are related by time-reversal symmetry. Therefore, $\alpha_z^x = \alpha_z \chi$. Space inversion symmetry is absent because, if the two valleys were related by it, $\Omega_{\mathbf{p}}^x$ would have the same sign on them. In addition, the model and the FS boundary conditions display a mirror symmetry \mathcal{M}_z about a plane perpendicular to z .

We compute $j_{2,x}^x(z)$, the contribution from valley χ to the nonlinear part of the longitudinal current, by combining Eqs. (14), (11) and (4). To zeroth order in α_z , we obtain [19]

$$j_{2,x}^x(z) \simeq \chi E_x^2 \frac{e^3}{8\pi^2 \hbar \varepsilon_F^2} \frac{m}{\int_0^\pi \frac{d\theta}{\tan^2 \theta}} \times \left[\left(z + \frac{a}{2} \right) e^{-\frac{z+a/2}{l \sin \theta}} - \left(-z + \frac{a}{2} \right) e^{-\frac{-z+a/2}{l \sin \theta}} \right], \quad (15)$$

where $l = c\tau(1 - m^2/\varepsilon_F^2)^{1/2}$ is an effective bulk mean free path due to impurity scattering.

Four properties of Eq. (15) are worth mentioning. First, $j_{2,x}^+(z) = j_{2,x}^+(-z)$, which is a consequence of the mirror symmetry \mathcal{M}_z . The same property is satisfied at first order in E_x , i.e. $j_{1,x}^+(z) = j_{1,x}^+(-z)$. As a

consequence, $j_x(z) = \sum_{\chi} j_x^{\chi}(z) = j_x(-z)$ at all orders in E_x , which is expected because an electric field along x preserves \mathcal{M}_z .

Second, $j_{2,x}^{\chi}(z) = -j_{2,x}^{\chi}(-z)$. This property can be understood mathematically from the fact that, in the absence of a tilt, the electronic dispersion (13) and the Berry curvature (14) of each valley are invariant under $(x, z; p_x, p_z) \rightarrow (-x, -z; -p_x, -p_z)$. Under this operation, $j_{2,x}^{\chi}(z) = \sigma_2 E_x^2 \rightarrow -j_{2,x}^{\chi}(-z) = \sigma_2' E_x^2$. From Neumann's principle [24], $\sigma_2 = \sigma_2'$ and therefore $j_{2,x}^{\chi}(z) = -j_{2,x}^{\chi}(-z)$. In contrast, $j_{1,x}^{\chi}(z) = \sigma_1 E_x \rightarrow -j_{1,x}^{\chi}(-z) = \sigma_1'(-E_x)$. Here, the symmetry condition $\sigma_1 = \sigma_1'$ leads to $j_{1,x}^{\chi}(z) = j_{1,x}^{\chi}(-z)$.

Third, $j_{2,x}^{\chi}(z)$ is localized near the edges of the wire. Such localization is directly associated to the second property, $j_{2,x}^{\chi}(z) = -j_{2,x}^{\chi}(-z)$. Indeed, far from the wire edges, the current density is expected to be spatially uniform and thus independent of z ; the relation $j_{2,x}^{\chi}(z) = -j_{2,x}^{\chi}(-z)$ then results in $j_{2,x}^{\chi} = -j_{2,x}^{\chi} = 0$ far from the edges. We emphasize that this localization of $j_{2,x}(z)$ near the edges takes place for bulk electrons, as our theory does not contain electronic surface states. In addition, the localization length for $j_{2,x}^{\chi}(z)$ is of the order of the bulk mean free path, unlike what one would expect from surface-states. Such spatial distribution of $j_{2,x}^{\chi}(z)$ is contrary to that of $j_{1,x}^{\chi}(z)$: at first order in E_x , the current is distributed along the entire bulk of the wire (even far from the edges, as allowed by relation $j_{1,x}^{\chi}(z) = j_{1,x}^{\chi}(-z)$) and partially depleted at the surfaces of the wire due to diffusive scattering therein.

Fourth, $j_{2,x}^{\chi}(z)$ is equal in magnitude and opposite in sign for the two valleys. This is an immediate joint consequence of the first two properties. Therefore, $j_{2,x}(z) = \sum_{\chi} j_{2,x}^{\chi}(z) = 0$ for all z . This is again different to the situation at first order in E_x , where $j_{1,x}^{\chi}(z) = j_{1,x}^{\chi}(-z)$ and hence the two valleys contribute with equal magnitude and sign when $\alpha_z = 0$.

A physical picture for the second and third properties is sketched in Fig. 1. The Berry curvature leads to an anomalous velocity $\propto E_x \Omega_{\mathbf{p},y}^{\chi}$ along the z direction for electrons of momentum \mathbf{p} at valley χ . Consequently, the term $E_x \Omega_{\mathbf{p},y}^{\chi} \partial_z f_{1,\mathbf{p}}^{\chi}$ in Eq. (10) describes the leading order contribution of the anomalous velocity to the divergence of the electronic current density ($f_{1,\mathbf{p}}^{\chi}$ appears to leading order, because $\partial_z f_{0,\mathbf{p}}^{\chi} = 0$). Here, the word ‘‘contribution’’ is to be emphasized, as the total current density along z is zero (i.e., the integral of $E_x \Omega_{\mathbf{p},y}^{\chi} f_{1,\mathbf{p}}^{\chi}$ over \mathbf{p} vanishes). But, if we focus on electrons with momentum \mathbf{p} , their flow has a nonzero divergence in the vicinity of the wire edges (the flow is divergenceless far from the edges because $\partial_z f_1^{\chi} \simeq 0$ therein according to Eq. (8)). This implies an accumulation of electrons of a given \mathbf{p} near the wire edges.

To determine the nature of such accumulation, we notice that (i) for fixed p_z , $f_{1,\mathbf{p}}^{\chi}$ has opposite sign for $p_x > 0$ and $p_x < 0$ (this is expected as there is a net electric current along x at first order in E_x); (ii)

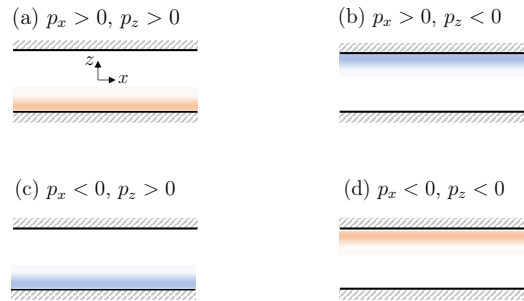


FIG. 1. Schematic contribution of the anomalous velocity to the electronic distribution function at a single valley of a 2D metal, as a function of the electronic momenta (p_x, p_z) . Orange: accumulation; blue: depletion; white: negligible contribution. Black solid lines denote the surfaces of the wire; grey dashed lines denote regions outside the wire. Regardless of p_z , there is an excess of right-moving electrons ($p_x > 0$) on one side of the wire and an excess of left-moving electrons ($p_x < 0$) on the opposite side of the wire.

for $p_z > 0$, $\partial_z f_{1,\mathbf{p}}^{\chi}$ is nonzero only near $z = -a/2$, while for $p_z < 0$, $\partial_z f_{1,\mathbf{p}}^{\chi}$ is nonzero only near $z = a/2$ (cf. Eq. (8)); (iii) for fixed p_x , $\partial_z f_{1,\mathbf{p}}^{\chi}$ switches sign under $p_z \rightarrow -p_z$ (this is again a consequence of the FS boundary conditions). It follows from (i), (ii) and (iii) that electrons with $p_x > 0$ and $p_x < 0$ accumulate on opposite edges of the wire (cf. Fig. 1). The accumulation takes place at order E_x^2 (one factor of E_x comes from the anomalous velocity, and the other from the spatial gradient of the electronic distribution function caused by diffusive boundary scattering). This is equivalent to a current distribution, which is quadratic in E_x , localized at the surfaces of the wires and antisymmetric with respect to the center of the wire. Hence, the second and third properties mentioned above are realized.

The presence of a tilt of the electronic structure along p_z changes some of the preceding properties qualitatively. Crucially, $\alpha_z \neq 0$ breaks the antisymmetry of $j_{2,x}^{\chi}(z)$ about the center of the wire (see Fig. 2). This is because $(x, z; p_x, p_z) \rightarrow (-x, -z; -p_x, -p_z)$ is no longer a symmetry when $\alpha_z \neq 0$. As a result, the two valleys no longer make mutually cancelling contributions to the nonlinear longitudinal current and $j_{2,x}(z)$ becomes nonzero. The relations $j_{n,x}^+(z) = j_{n,x}^-(z)$ and $j_{n,x}(z) = j_{n,x}(-z)$ continue to hold for $n = 1, 2$ because the tilt along p_z preserves the mirror symmetry \mathcal{M}_z . Also, $j_{n,x}^{\chi}(z)$ and by extension $j_{2,x}(z)$ continue to be localized near the wire surfaces. In Ref. [19], we show an expression for $j_{2,x}(z)$ that is valid up to first order in α_z/c . This term scales as the product of α_z and the Berry curvature.

Combining the expression for $j_{2,x}(z)$ in [19] with Eq. (6), we obtain the nonlinear part of the current density averaged over the thickness of the wire:

$$\overline{j_{2,x}} = \overline{\sigma_2} E_x^2 \simeq j_{2D} (1 - I), \quad (16)$$

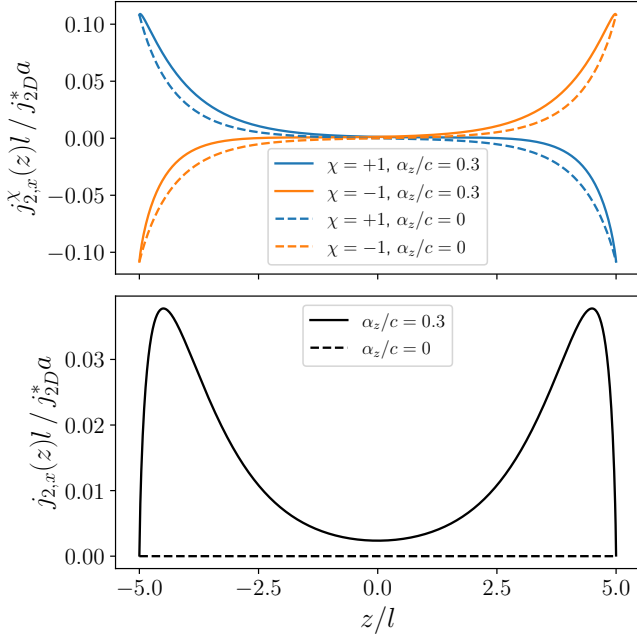


FIG. 2. Nonlinear longitudinal current density caused by the Berry curvature in a time-reversal-symmetric 2D Dirac metal with two electronic valleys ($\chi = \pm 1$). We take $a = 10l$ and $m = 0.5\varepsilon_F$. A tilt-independent normalization current $j_{2D}^* = j_{2D}c/\alpha_z$ is introduced, where j_{2D} is defined in the main text. (a) The valley-resolved current density $j_{2,x}^{\chi}(z)$ is localized near the wire edges, with a localization length of the order of l . In the absence of a tilt of the energy dispersion in the z direction ($\alpha_z = 0$), $j_{2,x}^{\chi}(z)$ is antisymmetric with respect to the center of the wire, and takes opposite values for the two valleys. A tilt $\alpha_z \neq 0$ skews the current density profile and prevents the cancellation between the two valleys. (b) The valley-summed nonlinear longitudinal current density $j_{2,x}(z)$ vanishes at every z when $\alpha_z = 0$. When $\alpha_z \neq 0$, $j_{2,x}(z)$ is nonzero and localized at the wire edges.

where

$$I = \frac{3}{8} \int_0^{\pi} d\theta \frac{\cos^2 \theta}{\sin \theta} \left(\frac{a}{l} + 2 \sin \theta \right)^2 \exp \left(-\frac{a}{l \sin \theta} \right) \quad (17)$$

is a dimensionless integral and

$$j_{2D} \equiv E_x^2 \frac{16e^3}{3\pi h} \frac{ml^2}{a\varepsilon_F^2} \sqrt{1 - \frac{m^2}{\varepsilon_F^2} \frac{\alpha_z}{c}} \quad (18)$$

is proportional to the Berry curvature evaluated at the Fermi energy [19]. This current reverses sign when the operation of time-reversal is applied to the system via $\alpha_z \rightarrow -\alpha_z$, $m \rightarrow -m$, $\tau \rightarrow -\tau$, $c \rightarrow -c$, with the other quantities remaining invariant. According to conventional knowledge [25], there should not exist a current proportional to τ^2 in a crystal with time-reversal symmetry, at least if skew-scattering is ignored [22]. Yet, such statement is no longer applicable when the electronic occupation varies in space, like in our case.

Analytical expressions of Eq. (16) are accessible in limiting regimes:

$$\overline{j_{2,x}} \simeq \begin{cases} j_{2D} & , a \gg l \\ 9a^2/(4l^2) \ln(l/a) j_{2D} & , a \ll l. \end{cases} \quad (19)$$

The fact that $\overline{\sigma_2} \propto 1/a$ when $a \gg l$ reflects the spatial localization of $j_{2,x}(z)$ near the wire edges, with a localization length that is independent of a . Thus, $\overline{\sigma_2} \rightarrow 0$ when $a \rightarrow \infty$. Likewise, $\overline{\sigma_2} \rightarrow 0$ in the $a \rightarrow 0$ limit, when the diffusive boundary scattering becomes pervasive. Given that $\overline{j_{2,x}}$ vanishes when $a \rightarrow 0$ and $a \rightarrow \infty$, it must have a maximum somewhere in between. The maximum of $\overline{\sigma_2}$, of value $\sim j_{2D}/E_x^2$, takes place at $a \sim l$. For $a \sim l$, $m \simeq 100\text{meV}$, $c \simeq 10^3\text{m/s}$ and $\alpha_z/c \simeq 0.3$, we find $\overline{\sigma_2}/\overline{\sigma_1} \simeq 10^{-3} \mu\text{m.volt}^{-1}$ [26]. Such ratio is similar to the one reported in the nonlinear Hall conductivity experiments (with the important difference that σ_2 is a longitudinal conductivity in our case).

Three dimensional Weyl metal.— Next, we consider a Weyl semimetal (WSM) [27] thin film in the xy plane, with $x, y \in (-\infty, \infty)$, and $z \in [-a/2, a/2]$. We start with two valleys of opposite chirality $\chi = \pm 1$, related by an improper crystal symmetry. We suppose that the Fermi energy ε_F intersects the conduction band. The electronic dispersion at valley χ is approximated as

$$\varepsilon_{\mathbf{p}}^{\chi} = cp + \alpha_y^{\chi} p_y + \alpha_z^{\chi} p_z, \quad (20)$$

where c is the Fermi velocity, $\mathbf{p} = (p_x, p_y, p_z)$ is the momentum measured from the Weyl point, α_y^{χ} and α_z^{χ} are tilt velocities at valley χ in the y and z directions, respectively. The Berry curvature for this model reads

$$\Omega_{\mathbf{p}}^{\chi} = \chi \hbar^2 \mathbf{p} / (2p^3). \quad (21)$$

Combining Eqs. (21), (11) and (4), we compute $j_{2,x}^{\chi}(z)$ [19]. Like in two dimensions, $j_{2,x}^{\chi}(z)$ is exponentially localized at the boundaries of the wire. In addition, if $\alpha_z^{\chi} = 0$, we find $j_{2,x}^{\chi}(z) = -j_{2,x}^{\chi}(-z)$, once again like in the 2D Dirac metal. We notice, however, that $\alpha_z^{\chi} \neq 0$ is necessary for $j_{2,x}^{\chi}(z) \neq 0$, because $\Omega_{\mathbf{p},y}^{\chi}$ is an odd function of p_y in a Weyl semimetal.

Averaging the current density over the wire thickness, we get $\overline{j_{2,x}} = 0$ when either α_y^{χ} or α_z^{χ} are zero [19]. Thus, it is required that the Weyl cones be tilted in both directions transverse to the transport direction. This is analogous to what we found for a two dimensional Dirac metal. The two valleys make perfectly cancelling contributions to $\overline{j_{2,x}}$ if $\alpha_y^{\chi} \alpha_z^{\chi}$ is independent of χ ; such is the case when the two valleys are related to one another by a mirror plane perpendicular to the x -axis ($\alpha_z^+ = -\alpha_z^-$ and $\alpha_y^+ = -\alpha_y^-$). If the two valleys are instead related by a mirror plane perpendicular to the z axis, then we have $\alpha_z^+ = -\alpha_z^-$ and $\alpha_y^+ = \alpha_y^-$. In such case, $j_{2,x}^+(z) = j_{2,x}^-(z)$ and $\overline{j_{2,x}} \neq 0$.

In thick and thin films, we get

$$\overline{j_{2,x}} \simeq \begin{cases} j_{3D} & , a \gg l \\ 3a^2/(2l^2) \ln(l/a) j_{3D} & , a \ll l \end{cases} \quad (22)$$

to leading order in $|\alpha_y^x|/c$ and $|\alpha_z^x|/c$, with

$$j_{3D} \equiv E_x^2 \frac{e^3 l^2}{12 a h^2 c} \sum_x \chi \frac{\alpha_y^x \alpha_z^x}{c^2}. \quad (23)$$

Thus, $\overline{j_{2,x}}$ vanishes when $a \rightarrow \infty$ and $a \rightarrow 0$, its maximum of value $j_{3D}/2$ occurring when $a \sim 0.5l$. For $\alpha_z^x/c \simeq 0.3\chi$, $\alpha_y^x/c \simeq 0.3$ and $a \simeq 0.5l$, we get $\overline{\sigma}_2 \simeq 10^{-6} l [\text{nm}] \text{ohm}^{-1} \text{volt}^{-1}$. In comparison, a nonlinear longitudinal conductivity of $10^{-3} \text{ohm}^{-1} \text{volt}^{-1}$ has been recently measured in chiral tellurium [28].

The preceding analysis can be extended to WSM with multiple pairs of valleys. For example, in a WSM with time-reversal symmetry, valleys related by time-reversal have opposite tilts but the same chirality. Based on Eq. (23), those valleys make equal contributions to $\overline{j_{2,x}}$, thereby enhancing it.

Conclusion.— We have unveiled a mechanism for a nonlinear longitudinal current in non-magnetic wires of finite thickness, resulting from (i) non-specular scattering of bulk electrons at wire surfaces; (ii) a Berry curvature in the direction orthogonal to both the transport and the

wire surface; (iii) an energy dispersion that is asymmetric at each electronic valley along the directions orthogonal to transport. Conditions (i) and (ii) ensure a current distribution that is quadratic in the applied electric field, parallel to the field, and localized in the vicinity of the surfaces. Condition (iii) enables a nonzero average of the nonlinear current density over the thickness of the wire. Skew-scattering and side-jump are not required.

We have illustrated our theory for Dirac and Weyl materials, where the effect appears to be sizeable. An experimental challenge is to distinguish the current predicted here from more conventional [22] but symmetry-allowed nonlinear currents. Possible strategies include thickness- and electron-density-dependent conductance measurements or the use of local current probes.

Acknowledgements.— This work has been financially supported by the Canada First Research Excellence Fund, the Natural Sciences and Engineering Research Council of Canada (Grant No. RGPIN- 2018-05385). We are grateful to C.-T. Chen, E. Lantagne-Hurtubise and A.-M. Tremblay for informative discussions.

-
- [1] D. Gall, *Journal of Applied Physics* **127**, 050901 (2020).
 [2] D. Gall, J. J. Cha, Z. Chen, H.-J. Han, C. Hinkle, J. A. Robinson, R. Sundararaman, and R. Torsi, *MRS Bulletin*, 1 (2021).
 [3] C. Zhang, Z. Ni, J. Zhang, X. Yuan, Y. Liu, Y. Zou, Z. Liao, Y. Du, A. Narayan, H. Zhang, *et al.*, *Nature materials* **18**, 482 (2019).
 [4] M. Breitzkreuz and P. W. Brouwer, *Phys. Rev. Lett.* **123**, 066804 (2019).
 [5] M. J. Gilbert, *Communications Physics* **4**, 70 (2021).
 [6] N. A. Lanzillo, U. Bajpai, I. Garate, and C.-T. Chen, *Physical Review Applied* **18**, 034053 (2022).
 [7] S.-W. Lien, I. Garate, U. Bajpai, C.-Y. Huang, C.-H. Hsu, Y.-H. Tu, N. A. Lanzillo, A. Bansil, T.-R. Chang, G. Liang, *et al.*, *npj Quantum Materials* **8**, 3 (2023).
 [8] K. Fuchs, *Mathematical Proceedings of the Cambridge Philosophical Society* **34**, 100 (1938).
 [9] E. H. Sondheimer, *Advances in Physics* **1**, 1 (1952).
 [10] I. Sodemann and L. Fu, *Physical review letters* **115**, 216806 (2015).
 [11] C. Ortix, *Advanced Quantum Technologies* **4**, 2100056 (2021).
 [12] Q. Ma, S.-Y. Xu, H. Shen, D. MacNeill, V. Fatemi, T.-R. Chang, A. M. Mier Valdivia, S. Wu, Z. Du, C.-H. Hsu, *et al.*, *Nature* **565**, 337 (2019).
 [13] K. Kang, T. Li, E. Sohn, J. Shan, and K. F. Mak, *Nature materials* **18**, 324 (2019).
 [14] Q. Ma, A. G. Grushin, and K. S. Burch, *Nature materials* **20**, 1601 (2021).
 [15] S. Tsirkin and I. Souza, *SciPost Physics Core* **5**, 039 (2022).
 [16] K. Das, S. Lahiri, R. B. Atencia, D. Culcer, and A. Agarwal, *Physical Review B* **108**, L201405 (2023).
 [17] Y. Wang, Z. Zhang, Z.-G. Zhu, and G. Su, “An intrinsic nonlinear ohmic current,” (2023), [arXiv:2207.01182](https://arxiv.org/abs/2207.01182) [[cond-mat.mes-hall](https://arxiv.org/abs/2207.01182)].
 [18] D. Xiao, Y. Yao, Z. Fang, and Q. Niu, *Physical Review Letters* **97**, 026603 (2006).
 [19] See Supplemental Material at [URL] for details of the analytical derivations and citations [29, 30].
 [20] We have omitted any hypothetical internal electric field component in the z direction. In systems displaying a nonlinear Hall effect, an internal nonzero E_z would emerge, which would be quadratic in E_x . However, the source term produced by such a field in Eq. (10) would be even in p_x and hence irrelevant for transport along x .
 [21] This statement, which we have verified within the RTA, is in agreement with conventional theories [25].
 [22] H. Isobe, S.-Y. Xu, and L. Fu, *Science advances* **6**, eaay2497 (2020).
 [23] D. Xiao, M.-C. Chang, and Q. Niu, *Reviews of modern physics* **82**, 1959 (2010).
 [24] R. C. Powell, *Symmetry, Group Theory, and the Physical Properties of Crystals*, Lecture Notes in Physics, Vol. 824 (Springer New York, New York, NY, 2010).
 [25] Y. Gao, *Frontiers of Physics* **14**, 1 (2019).
 [26] To leading order in α_z , $\overline{\sigma}_2/\overline{\sigma}_1 \simeq eh\alpha_z/(6\pi m^2)$ for $a \simeq l$.
 [27] N. Armitage, E. Mele, and A. Vishwanath, *Reviews of Modern Physics* **90**, 015001 (2018).
 [28] M. Suárez-Rodríguez, B. Martín-García, W. Skowroński, F. Calavalle, S. S. Tsirkin, I. Souza, F. De Juan, A. Chuvilin, A. Fert, M. Gobbi, F. Casanova, and L. E. Hueso, *Phys. Rev. Lett.* **132**, 046303 (2024).
 [29] A. M. Tremblay, B. Patton, P. C. Martin, and P. F. Maldague, *Phys. Rev. A* **19**, 1721 (1979).
 [30] A.-M. S. Tremblay and F. Vidal, *Phys. Rev. B* **25**, 7562 (1982).

Appendix A: Details about the solution of the Boltzmann equation

The Boltzmann equation we wish to solve has the form

$$v_{\mathbf{p}}^{\chi} \frac{\partial f_{\mathbf{p}}^{\chi}}{\partial z} - eE_x \frac{\partial f_{\mathbf{p}}^{\chi}}{\partial p_x} = -\frac{1}{\tau} \left(f_{\mathbf{p}}^{\chi} - \frac{1}{\rho(\varepsilon_{\mathbf{p}}^{\chi})} \sum_{\mathbf{p}'} f_{\mathbf{p}'}^{\chi} \delta(\varepsilon_{\mathbf{p}} - \varepsilon_{\mathbf{p}'}) \right), \quad (\text{A1})$$

where τ is the elastic scattering time (assumed to be a constant), $\rho(\varepsilon)$ is the electronic density of states at energy ε and the sum over \mathbf{p}' is confined to the valley χ . Without inelastic scattering, steady state is reached only in the presence of a temperature gradient, needed to evacuate the Joule heating produced by the current [29, 30]. This temperature gradient is quadratic in E_x and influences the part of the electron occupation that is isotropic in momentum. It will therefore not affect our calculation of the current and we will hence ignore it.

We solve Eq. (A1) perturbatively in powers of E_x up to second order, $f_{\mathbf{p}}^{\chi} \simeq f_{0,\mathbf{p}}^{\chi} + f_{1,\mathbf{p}}^{\chi} + f_{2,\mathbf{p}}^{\chi}$, where $f_{n,\mathbf{p}}^{\chi} \propto E_x^n$. We wish to avoid using the relaxation time approximation, which leads to a violation of conservation laws. We are able to do so, at the expense of introducing some simplifying assumptions.

To first order in E_x , Eq. (A1) reads

$$v_z^{\chi} \frac{\partial f_{1,\mathbf{p}}^{\chi}}{\partial z} - eE_x \frac{\partial f_{0,\mathbf{p}}^{\chi}}{\partial p_x} = -\frac{1}{\tau} \left(f_{1,\mathbf{p}}^{\chi} - \frac{1}{\rho(\varepsilon_{\mathbf{p}}^{\chi})} \sum_{\mathbf{p}'} f_{1,\mathbf{p}'}^{\chi} \delta(\varepsilon_{\mathbf{p}} - \varepsilon_{\mathbf{p}'}) \right). \quad (\text{A2})$$

To make further progress, we assume that $\varepsilon_{\mathbf{p}}^{\chi}$ is invariant under $p_x \rightarrow -p_x$. Then, the second term in left hand side in Eq. (A2), which acts as a source term for $f_{1,\mathbf{p}}^{\chi}$, is an odd function of p_x . As a result, if we make an ansatz of separating $f_{1,\mathbf{p}}^{\chi}$ into a part that is even in p_x and a part that is odd in p_x , then the even part can be taken to be equal to zero. For the odd part, $f_{1,\mathbf{p}}^{\chi,o}$, Eq. (A2) becomes

$$v_z^{\chi} \frac{\partial f_{1,\mathbf{p}}^{\chi,o}}{\partial z} - eE_x \frac{\partial f_{0,\mathbf{p}}^{\chi}}{\partial p_x} = -\frac{1}{\tau} f_{1,\mathbf{p}}^{\chi,o}. \quad (\text{A3})$$

The solution of this equation with the boundary condition of Fuchs and Sondheimer yields Eq. (8) of the main text.

To second order in E_x , Eq. (A1) reads

$$v_z^{\chi} \frac{\partial f_{2,\mathbf{p}}^{\chi}}{\partial z} - eE_x \frac{\partial f_{1,\mathbf{p}}^{\chi}}{\partial p_x} + \frac{eE_x \Omega_{\mathbf{p},y}^{\chi}}{\hbar} \frac{\partial f_{1,\mathbf{p}}^{\chi}}{\partial z} = -\frac{1}{\tau} \left(f_{2,\mathbf{p}}^{\chi} - \frac{1}{\rho(\varepsilon_{\mathbf{p}})} \sum_{\mathbf{p}'} f_{2,\mathbf{p}'}^{\chi} \delta(\varepsilon_{\mathbf{p}} - \varepsilon_{\mathbf{p}'}) \right). \quad (\text{A4})$$

To solve this, we again assume that $\varepsilon_{\mathbf{p}}^{\chi}$ is invariant under $p_x \rightarrow -p_x$. Then, the second and third terms in Eq. (A4) are even and odd functions of p_x , respectively (in the models we consider, $\Omega_{\mathbf{p},y}^{\chi}$ is an even function of p_x). As such, if we once again decompose $f_{2,\mathbf{p}}^{\chi}$ into a part that is even in p_x ($f_{2,\mathbf{p}}^{\chi,e}$) and a part that is odd in p_x ($f_{2,\mathbf{p}}^{\chi,o}$), then Eq. (A4) gives

$$v_z^{\chi} \frac{\partial f_{2,\mathbf{p}}^{\chi,e}}{\partial z} - eE_x \frac{\partial f_{1,\mathbf{p}}^{\chi}}{\partial p_x} = -\frac{1}{\tau} \left(f_{2,\mathbf{p}}^{\chi,e} - \frac{1}{\rho(\varepsilon_{\mathbf{p}})} \sum_{\mathbf{p}'} f_{2,\mathbf{p}'}^{\chi,e} \delta(\varepsilon_{\mathbf{p}} - \varepsilon_{\mathbf{p}'}) \right), \quad (\text{A5})$$

$$v_z^{\chi} \frac{\partial f_{2,\mathbf{p}}^{\chi,o}}{\partial z} + \frac{eE_x \Omega_{\mathbf{p},y}}{\hbar} \frac{\partial f_{1,\mathbf{p}}^{\chi}}{\partial z} = -\frac{f_{2,\mathbf{p}}^{\chi,o}}{\tau}. \quad (\text{A6})$$

The equation for $f_{2,\mathbf{p}}^{\chi,o}$ can be easily solved together with the Fuchs-Sondheimer boundary conditions; the solution is shown in Eq. (11) of the main text. In contrast, the equation for $f_{2,\mathbf{p}}^{\chi,e}$ is not amenable to an analytical solution. Yet, this part is not relevant to the calculation of the electric current density in Eq. (4) of the main text.

Appendix B: Derivation of the nonlinear current density in a two-dimensional Dirac metal

In this Appendix, we calculate the part of the current density that is quadratic in the applied electric field, in a toy model for a 2D Dirac metal with time reversal symmetry and nonzero Berry curvature. The starting point is

$$j_{2,x}(z) = -\frac{e}{(2\pi\hbar)^2} \sum_{\chi} \int dp_x dp_z v_x^{\chi} f_{2,\mathbf{p}}^{\chi}, \quad (\text{B1})$$

where $f_{2,\mathbf{p}}^X$ is the quadratic-in- E_x part of the electronic distribution. Assuming that the energy dispersion is symmetric under $p_x \rightarrow -p_x$, $f_{2,\mathbf{p}}^X$ is given by Eq. (11) of the main text. Because $f_{2,\mathbf{p}}^X$ is strongly peaked at the Fermi energy, the integral over p_x and p_z can be extended from $-\infty$ to $+\infty$ on each valley. In addition, because the form of $f_{2,\mathbf{p}}^X$ depends on the sign of v_z^X , it is mathematically convenient to change the integration variables from $\{p_x, p_z\}$ to $\{v_x, v_z\}$ using the relations

$$p_x = \frac{mv_x}{c\sqrt{c^2 - v_x^2 - (v_z - \chi\alpha_z)^2}}, \quad p_z = \frac{m(v_z - \chi\alpha_z)}{c\sqrt{c^2 - v_x^2 - (v_z - \chi\alpha_z)^2}}, \quad (\text{B2})$$

where we hereafter omit the superscript χ in v_x and v_z . The arguments of the square roots of Eq. (B2) must be positive. The Jacobian of the transformation reads

$$JX = \left| \begin{array}{cc} \frac{\partial p_x}{\partial v_x} & \frac{\partial p_x}{\partial v_z} \\ \frac{\partial p_z}{\partial v_x} & \frac{\partial p_z}{\partial v_z} \end{array} \right| = \frac{m^2}{[v_x^2 + (v_z - \chi\alpha_z)^2 - c^2]^2}. \quad (\text{B3})$$

Therefore, the nonlinear part of the current density is given by

$$\begin{aligned} j_{2,x}(z) &= -\frac{e}{(2\pi\hbar)^2} \sum_{\chi} \int dv_x dv_z v_x JX f_2^X \\ &= -\frac{e}{(2\pi\hbar)^2} \sum_{\chi} \int dv_x v_x \left(\int_{v_z < 0} dv_z JX f_2^X + \int_{v_z > 0} dv_z JX f_2^X \right), \end{aligned} \quad (\text{B4})$$

where we have divided the last integral in two parts because f_2^X has different expressions for $v_z > 0$ and $v_z < 0$.

Assuming that $|\alpha_z| \ll c$, the electronic dispersion is close to being isotropic and thus it is convenient to do the integration in Eq. (B4) in polar coordinates, ($v_x = v \cos \theta$, $v_z = v \sin \theta$, $dv_x dv_z = v dv d\theta$). Then,

$$\begin{aligned} j_{2,x}(z) &= -\frac{e^3 E_x^2}{\hbar(2\pi\hbar)^2} \sum_{\chi} \int_0^{\infty} dv \left(-\int_{\pi}^{2\pi} d\theta \frac{\cos \theta}{\sin^2 \theta} JX \frac{\partial f_0^X}{\partial p_x} \Omega_{\mathbf{p},y}^X (a-z) e^{(a-z)/\tau v \sin \theta} \right. \\ &\quad \left. + \int_0^{\pi} d\theta \frac{\cos \theta}{\sin^2 \theta} JX \frac{\partial f_0^X}{\partial p_x} \Omega_{\mathbf{p},y}^X z e^{-z/\tau v \sin \theta} \right), \end{aligned} \quad (\text{B5})$$

where the Berry curvature in the valley χ reads

$$\Omega_{\mathbf{p},y}^X = \chi \frac{m\hbar^2 c^2}{2(c^2 p^2 + m^2)^{3/2}} = \chi \frac{m\hbar^2 c^2}{2(\varepsilon_{\mathbf{p}}^X - \chi\alpha_z p_z)^3}. \quad (\text{B6})$$

Since $\partial f_0^X / \partial p_x$ is peaked at the Fermi energy, we can approximate $\varepsilon_{\mathbf{p}}^X \approx \varepsilon_F$ inside the integral, and then develop the Berry curvature up to the first order in α_z (because $|\alpha_z p_z| \ll \varepsilon_F$ at the Fermi surface). We obtain

$$\Omega_{\mathbf{p},y}^X \simeq \chi \frac{m\hbar^2 c^2}{2\varepsilon_F^3} \left(1 + \chi \frac{3\alpha_z p_z}{\varepsilon_F} \right) = \chi \frac{m\hbar^2 c^2}{2\varepsilon_F^3} + \chi^2 \frac{3m\hbar^2 c^2}{2\varepsilon_F^4} \alpha_z p_z \equiv \Omega_y^X \left(1 + 3\chi \frac{\alpha_z p_z}{\varepsilon_F} \right), \quad (\text{B7})$$

where $\Omega_y^X \equiv \chi \Omega_{\mathbf{p},y}^X = \chi \frac{m\hbar^2 c^2}{2\varepsilon_F^3}$ is the Berry curvature without any tilt in the dispersion. In polar coordinates,

$$\Omega_{\mathbf{p},y}^X \simeq \Omega_y^X \left(1 + 3\chi \frac{m}{\varepsilon_F} \frac{v \sin \theta}{(c^2 - v^2)^{1/2}} \frac{\alpha_z}{c} \right). \quad (\text{B8})$$

In Eq. (B5), we have written the upper bound of v up as ∞ , in apparent contradiction with the fact that the square roots in Eq. (B2) must be positive. Yet, the fact that the derivative of the Fermi-Dirac distribution is peaked at the Fermi energy allows us to extend the upper bound of the v -integral. Indeed, at low temperature,

$$\frac{\partial f_0^X}{\partial p_x} = \frac{\partial f_0}{\partial \varepsilon_{\mathbf{p}}^X} \frac{\partial \varepsilon_{\mathbf{p}}^X}{\partial p_x} \approx -v \cos \theta \delta(\varepsilon_{\mathbf{p}}^X - \varepsilon_F), \quad (\text{B9})$$

where

$$\delta(\varepsilon_{\mathbf{p}}^X - \varepsilon_F) = \left| \frac{\partial \varepsilon_{\mathbf{p}}^X}{\partial v} \right|_{v=v_*^X}^{-1} \delta(v - v_*^X) \quad (\text{B10})$$

and v_*^χ is such that $\varepsilon_{\mathbf{p}}^\chi = \varepsilon_F$ when $v = v_*^\chi$. Expanding to first order in the tilt parameter α_z , we get

$$v_*^\chi \simeq c \sqrt{1 - \frac{m^2}{\varepsilon_F^2}} \left[1 + \chi \frac{\alpha_z}{c} \sqrt{1 - \frac{m^2}{\varepsilon_F^2}} \sin \theta \right]. \quad (\text{B11})$$

Insofar as the second term in the square brackets of Eq. (B11) is smaller than 1/2 in absolute value, the arguments of the square roots in Eq. (B2) are indeed positive. In addition, we get

$$\frac{\partial f_0^\chi}{\partial p_x} \simeq -\frac{vm^2c \cos \theta}{\varepsilon_F^3} \left(\frac{1}{\sqrt{1 - \frac{m^2}{\varepsilon_F^2}}} + 2\chi \frac{\alpha_z}{c} \sin \theta \right) \delta(v - v_*^\chi), \quad (\text{B12})$$

where again we neglect higher order terms in α_z/c . The Dirac delta function makes the integration over v in Eq. (B5) immediate. Afterwards, we expand the integrand up to first order in α_z . The outcome is

$$\begin{aligned} j_{2,x}(z) &= \frac{e^3 E_x^2}{\hbar(2\pi\hbar)^2} \frac{\varepsilon_F}{c^2} l \sum_\chi \Omega_y^\chi \int_0^\pi \frac{d\theta}{\tan^2 \theta} \left\{ \left[1 + \left(\frac{z+a/2}{l} + 2 \sin \theta \right) \sqrt{1 - \frac{m^2}{\varepsilon_F^2}} \frac{\alpha_z \chi}{c} \right] \frac{z+a/2}{l} e^{-\frac{z+a/2}{l \sin \theta}} \right. \\ &\quad \left. + \left[1 + \left(\frac{z-a/2}{l} - 2 \sin \theta \right) \sqrt{1 - \frac{m^2}{\varepsilon_F^2}} \frac{\alpha_z \chi}{c} \right] \frac{z-a/2}{l} e^{-\frac{-z+a/2}{l \sin \theta}} \right\} \\ &= \frac{2e^3 E_x^2 \Omega_y}{\hbar(2\pi\hbar)^2} \frac{\varepsilon_F}{c^2} l \sqrt{1 - \frac{m^2}{\varepsilon_F^2}} \frac{\alpha_z}{c} \int_0^\pi \frac{d\theta}{\tan^2 \theta} \left[\left(\frac{z+a/2}{l} + 2 \sin \theta \right) \frac{z+a/2}{l} e^{-\frac{z+a/2}{l \sin \theta}} \right. \\ &\quad \left. + \left(\frac{z-a/2}{l} - 2 \sin \theta \right) \frac{z-a/2}{l} e^{-\frac{-z+a/2}{l \sin \theta}} \right] \\ &\equiv \frac{2e^3 E_x^2 \Omega_y}{\hbar(2\pi\hbar)^2} \frac{\varepsilon_F}{c^2} l \sqrt{1 - \frac{m^2}{\varepsilon_F^2}} \frac{\alpha_z}{c} \mathcal{I}(z/l). \end{aligned} \quad (\text{B13})$$

Averaging $j_{2,x}(z)$ over the wire thickness,

$$\overline{j_{2,x}} = \frac{1}{a} \int_{-a/2}^{a/2} dz j_{2,x}(z), \quad (\text{B14})$$

using the property

$$\int_{-a/2}^{a/2} dz F(a/2 - z) = \int_{-a/2}^{a/2} dz F(z + a/2) \quad (\text{B15})$$

and following up with some algebraic manipulations, we arrive at

$$\begin{aligned} \overline{j_{2,x}} &= \frac{4e^3 E_x^2 \Omega_y}{\hbar(2\pi\hbar)^2} \frac{\varepsilon_F}{c^2} \frac{\alpha_z}{c} \sqrt{1 - \frac{m^2}{\varepsilon_F^2}} \frac{l^2}{a} \int_0^\pi d\theta \frac{\cos^2 \theta}{\sin \theta} \left(4 \sin^2 \theta - \left(\frac{a}{l} + 2 \sin \theta \right)^2 \exp \left(-\frac{a}{l \sin \theta} \right) \right) \\ &= \frac{32}{3} \frac{e^3 E_x^2 \Omega_y}{\hbar(2\pi\hbar)^2} \frac{\varepsilon_F}{c^2} \frac{\alpha_z}{c} \sqrt{1 - \frac{m^2}{\varepsilon_F^2}} \frac{l^2}{a} \left[1 - \frac{3}{8} \int_0^\pi d\theta \frac{\cos^2 \theta}{\sin \theta} \left(\frac{a}{l} + 2 \sin \theta \right)^2 \exp \left(-\frac{a}{l \sin \theta} \right) \right] \\ &\equiv j_{2\text{D}}(1 - I), \end{aligned} \quad (\text{B16})$$

which is the result quoted in the main text with

$$j_{2\text{D}} = \frac{32}{3} \frac{e^3 E_x^2 \Omega_y}{\hbar(2\pi\hbar)^2} \frac{\varepsilon_F}{c^2} \frac{\alpha_z}{c} \sqrt{1 - \frac{m^2}{\varepsilon_F^2}} \frac{l^2}{a} \quad \text{and} \quad I = \frac{3}{8} \int_0^\pi d\theta \frac{\cos^2 \theta}{\sin \theta} \left(\frac{a}{l} + 2 \sin \theta \right)^2 \exp \left(-\frac{a}{l \sin \theta} \right).$$

The averaged current is plotted in Fig. 3.

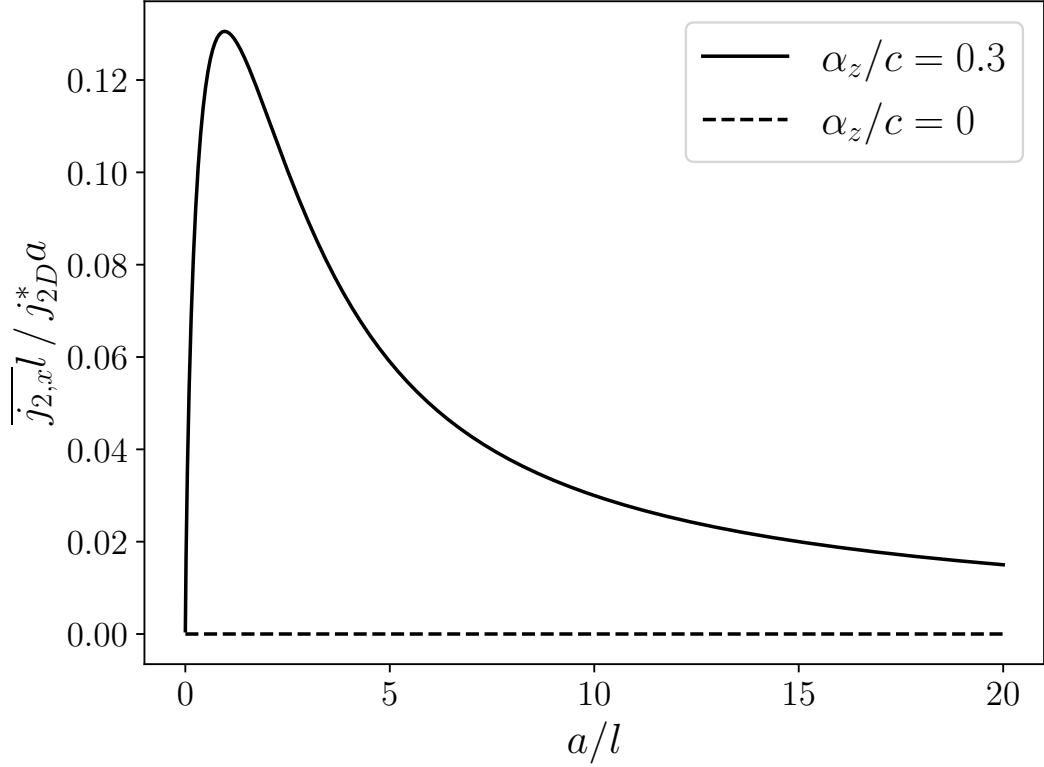


FIG. 3. Average nonlinear current density as a function of the wire thickness. A tilt-independent normalization current $j_{2D}^* = j_{2D}c/\alpha_z$ is introduced, j_{2D}^*a being independent of thickness. This figure shows that $\overline{j_{2,x}} \rightarrow 0$ when $a/l \rightarrow \infty$ and $a \rightarrow 0$, with a maximum that occurs when $a/l \approx 1$.

Appendix C: Derivation of the nonlinear current density in a three-dimensional Weyl semimetal

In this Appendix, we calculate the part of the current density that is quadratic in the applied electric field, in a toy model for a 3D Weyl semimetal. The expression for that current is

$$j_{2,x}(z) = -\frac{e}{(2\pi\hbar)^3} \sum_{\chi} \int dp_x dp_y dp_z \dot{x}_{\mathbf{p}}^{\chi} f_{2,\mathbf{p}}^{\chi}, \quad (\text{C1})$$

where, under the same assumptions of the preceding Appendix, $f_{2,\mathbf{p}}^{\chi}$ is given by Eq. (11) of the main text. Because $f_{2,\mathbf{p}}^{\chi}$ is strongly peaked at the Fermi energy, the integral over p_i can be extended from $-\infty$ to $+\infty$ on each valley.

Like in the previous Appendix, at first glance we are tempted to do a change of variables from (p_x, p_y, p_z) to $(v_x^{\chi}, v_y^{\chi}, v_z^{\chi})$, where $v_i^{\chi} = \partial_{p_i} \varepsilon_{\mathbf{p}}^{\chi}$. Yet, this change of variables is mathematically ill-defined, because the three velocities are not independent variables (e.g., $(v_x^{\chi})^2 + (v_y^{\chi})^2 + (v_z^{\chi})^2 = c^2$ in the case of an isotropic dispersion). Instead, we perform the following transformation:

$$\begin{pmatrix} p_x \\ p_y \\ p_z \end{pmatrix} \rightarrow \begin{pmatrix} p_{\parallel} \cos \phi \\ p_{\parallel} \sin \phi \\ v_z^{\chi} \end{pmatrix}. \quad (\text{C2})$$

The Jacobian of the transformation is

$$J^{\chi} = p_{\parallel} \left| \frac{\partial p_z}{\partial v_z^{\chi}} \right| = p_{\parallel} \left| \frac{\partial}{\partial v_z^{\chi}} \left(\frac{(v_z^{\chi} - \alpha_z^{\chi}) p_{\parallel}}{\sqrt{c^2 - (v_z^{\chi} - \alpha_z^{\chi})^2}} \right) \right| = \frac{p_{\parallel}^2 c^2}{[c^2 - (v_z^{\chi} - \alpha_z^{\chi})^2]^{3/2}}. \quad (\text{C3})$$

The current density is then written as

$$j_{2,x} = -\frac{e}{(2\pi\hbar)^3} \sum_{\chi} \int_0^{\infty} dp_{\parallel} \int_0^{2\pi} d\phi \left(\int_{-\infty}^0 dv_z^{\chi} \frac{v_x^{\chi} p_{\parallel}^2 c^2}{(c^2 - (v_z^{\chi} - \alpha_z^{\chi})^2)^{3/2}} f_2^{\chi} + \int_0^{\infty} dv_z^{\chi} \frac{v_x^{\chi} p_{\parallel}^2 c^2}{(c^2 - (v_z^{\chi} - \alpha_z^{\chi})^2)^{3/2}} f_2^{\chi} \right), \quad (\text{C4})$$

with the implicit constraint in the integrations over v_z^x that the argument of the square root in Eq. (C3) must be positive.

Let us take a closer look at the integrand of Eq. (C4). For $v_z^x > 0$, we have

$$-\frac{v_x^x p_{\parallel}^2 c^2}{(c^2 - (v_z^x - \alpha_z^x)^2)^{3/2}} \frac{e^2 E_x^2 \Omega_{\mathbf{p},y}^x (\partial_{p_x} f_0)(z + a/2) e^{-\frac{z+a/2}{v_z^x \tau}}}{\hbar (v_z^x)^2}, \quad (\text{C5})$$

where

$$\Omega_{\mathbf{p},y}^x = \chi \frac{\hbar^2 p_{\parallel} \sin \phi}{2(p_{\parallel}^2 + p_z^2)^{3/2}} \quad (\text{C6})$$

is the y -component of the Berry curvature. At low temperature,

$$\partial_{p_x} f_0 \simeq -v_x^x \delta(\varepsilon - \varepsilon_F) = -v_x^x \frac{\delta(p_{\parallel} - p_{\parallel}^*)}{\left| \frac{\partial \varepsilon}{\partial p_{\parallel}} \right|_{p_{\parallel}^*}}, \quad (\text{C7})$$

where p_{\parallel}^* is the value of p_{\parallel} such that $\varepsilon(p_{\parallel}^*, \phi, v_z^x) = \varepsilon_F$. We can also rewrite v_x^x as a function of the new variables as

$$v_x^x = \sqrt{c^2 - (v_z^x - \alpha_z^x)^2} \cos \phi. \quad (\text{C8})$$

Putting everything together and using

$$p_z = \frac{(v_z^x - \alpha_z^x) p_{\parallel}}{\sqrt{c^2 - (v_z^x - \alpha_z^x)^2}}, \quad (\text{C9})$$

the integrand for $v_z^x > 0$ becomes

$$-\chi \frac{e^2 E_x^2 \hbar}{2c(v_z^x)^2} \frac{\cos^2 \phi \sin \phi (c^2 - (v_z^x - \alpha_z^x)^2)^{3/2} \delta(p_{\parallel} - p_{\parallel}^*)}{c^2 + \alpha_y^x \sin \phi \sqrt{c^2 - (v_z^x - \alpha_z^x)^2} + \alpha_z^x (v_z^x - \alpha_z^x)} \left(z + \frac{a}{2} \right) e^{-(z+a/2)/\tau v_z^x}. \quad (\text{C10})$$

The integration of Eq. (C10) over p_{\parallel} and ϕ gives

$$-\chi \frac{e^2 E_x^2 \hbar}{2c(v_z^x)^2} \frac{(c^2 - (v_z^x - \alpha_z^x)^2)^{3/2}}{c^2 + \alpha_z^x (v_z^x - \alpha_z^x)} \left(z + \frac{a}{2} \right) e^{-(z+a/2)/\tau v_z^x} \int_0^{2\pi} d\phi \frac{\cos^2 \phi \sin \phi}{1 + b \sin \phi}, \quad (\text{C11})$$

where

$$b \equiv \frac{\alpha_y^x \sqrt{c^2 - (v_z^x - \alpha_z^x)^2}}{c^2 + \alpha_z^x (v_z^x - \alpha_z^x)} \quad (\text{C12})$$

and $c^2 - (v_z^x - \alpha_z^x)^2 > 0$ is required. The integral in Eq. (C11) has three possible solutions depending on the value of b ($|b| < 1$, $b = 1$, $|b| > 1$). When the tilts are small or moderate, $|b| < 1$ is the relevant regime and that is what we will focus on henceforth. Consequently, the result of the integral is

$$\int_0^{2\pi} d\phi \frac{\cos^2 \phi \sin \phi}{1 + b \sin \phi} = \frac{b^2 - 2 + 2\sqrt{1 - b^2}}{b^3} \pi. \quad (\text{C13})$$

Consequently, Eq. (C11) becomes

$$-\chi \frac{e^2 E_x^2 \hbar}{2c(v_z^x)^2} \frac{(c^2 - (v_z^x - \alpha_z^x)^2)^{3/2}}{c^2 + \alpha_z^x (v_z^x - \alpha_z^x)} \left(z + \frac{a}{2} \right) e^{-(z+a/2)/\tau v_z^x} \frac{b^2 - 2 + 2\sqrt{1 - b^2}}{b^3} \pi. \quad (\text{C14})$$

If $|\alpha_y^x| \ll c$, we may approximate

$$\frac{b^2 - 2 + 2\sqrt{1 - b^2}}{b^3} \pi \approx -\frac{\pi b}{4}, \quad (\text{C15})$$

by which Eq. (C11) simplifies to

$$\chi \frac{e^2 E_x^2 \hbar \pi}{8c} \frac{\alpha_y^\chi}{(v_z^\chi)^2} \left(\frac{c^2 - (v_z^\chi - \alpha_z^\chi)^2}{c^2 + \alpha_z^\chi (v_z^\chi - \alpha_z^\chi)} \right)^2 \left(z + \frac{a}{2} \right) e^{-(z+a/2)/\tau v_z^\chi}. \quad (\text{C16})$$

The treatment is exactly the same for $v_z^\chi < 0$ part of Eq. (C4). Putting everything together, the nonlinear current density for the valley χ reads

$$j_{2,x}^\chi(z) = -\chi \frac{e^3 E_x^2 \hbar \pi}{8c(2\pi\hbar)^3} \alpha_y^\chi \left\{ \int_{-c+\alpha_z^\chi}^0 dv_z^\chi \frac{1}{(v_z^\chi)^2} \left(\frac{c^2 - (v_z^\chi - \alpha_z^\chi)^2}{c^2 + \alpha_z^\chi (v_z^\chi - \alpha_z^\chi)} \right)^2 \left(z - \frac{a}{2} \right) e^{-(z-a/2)/\tau v_z^\chi} \right. \\ \left. + \int_0^{c+\alpha_z^\chi} dv_z^\chi \frac{1}{(v_z^\chi)^2} \left(\frac{c^2 - (v_z^\chi - \alpha_z^\chi)^2}{c^2 + \alpha_z^\chi (v_z^\chi - \alpha_z^\chi)} \right)^2 \left(z + \frac{a}{2} \right) e^{-(z+a/2)/\tau v_z^\chi} \right\}. \quad (\text{C17})$$

Defining the dimensionless quantities $(\tilde{\alpha}_{y,z}^\chi, \tilde{v}_z^\chi) = (\alpha_{y,z}^\chi, v_z^\chi)/c$ and $(\tilde{z}, \tilde{a}) = (z, a)/l$, with $l = c\tau$ as an effective bulk mean free path from impurity scattering, we have

$$j_{2,x}^\chi(\tilde{z}) = -\chi \frac{e^3 E_x^2 \hbar \pi l}{8c(2\pi\hbar)^3} \tilde{\alpha}_y^\chi \left\{ \int_0^{1+\tilde{\alpha}_z^\chi} d\tilde{v}_z^\chi \frac{1}{(\tilde{v}_z^\chi)^2} \left(\frac{1 - (\tilde{v}_z^\chi - \tilde{\alpha}_z^\chi)^2}{1 + \tilde{\alpha}_z^\chi (\tilde{v}_z^\chi - \tilde{\alpha}_z^\chi)} \right)^2 \left(\tilde{z} + \frac{\tilde{a}}{2} \right) e^{-(\tilde{z}+\tilde{a}/2)/\tilde{v}_z^\chi} \right. \\ \left. + \int_{-1+\tilde{\alpha}_z^\chi}^0 d\tilde{v}_z^\chi \left(\frac{1 - (\tilde{v}_z^\chi - \tilde{\alpha}_z^\chi)^2}{1 + \tilde{\alpha}_z^\chi (\tilde{v}_z^\chi - \tilde{\alpha}_z^\chi)} \right)^2 \left(\tilde{z} - \frac{\tilde{a}}{2} \right) e^{-(\tilde{z}-\tilde{a}/2)/\tilde{v}_z^\chi} \right\}. \quad (\text{C18})$$

If the two valleys are related by a mirror plane perpendicular to the z -axis ($\tilde{\alpha}_y^+ = \tilde{\alpha}_y^-$ and $\tilde{\alpha}_z^+ = -\tilde{\alpha}_z^-$), we have $j_{2,x}^+(\tilde{z}) = j_{2,x}^-(-\tilde{z})$.

Averaging Eq. (C17) over the wire thickness, we get

$$\overline{j_{2,x}^\chi} = -\chi \frac{e^3 E_x^2 \hbar \pi l}{8c(2\pi\hbar)^3} \frac{\tilde{\alpha}_y^\chi}{\tilde{a}} \left\{ \int_0^{1+\tilde{\alpha}_z^\chi} d\tilde{v}_z^\chi \left(\frac{1 - (\tilde{v}_z^\chi - \tilde{\alpha}_z^\chi)^2}{1 + \tilde{\alpha}_z^\chi (\tilde{v}_z^\chi - \tilde{\alpha}_z^\chi)} \right)^2 \left[1 - \left(1 + \frac{\tilde{a}}{\tilde{v}_z^\chi} \right) e^{-\tilde{a}/\tilde{v}_z^\chi} \right] \right. \\ \left. - \int_{-1+\tilde{\alpha}_z^\chi}^0 d\tilde{v}_z^\chi \left(\frac{1 - (\tilde{v}_z^\chi - \tilde{\alpha}_z^\chi)^2}{1 + \tilde{\alpha}_z^\chi (\tilde{v}_z^\chi - \tilde{\alpha}_z^\chi)} \right)^2 \left[1 - \left(1 - \frac{\tilde{a}}{\tilde{v}_z^\chi} \right) e^{\tilde{a}/\tilde{v}_z^\chi} \right] \right\}. \quad (\text{C19})$$

When $\tilde{a} \gg 1$, the preceding expression simplifies to

$$\overline{j_{2,x}^\chi} \simeq \chi E_x^2 \frac{e^3 l^2}{12ah^2c} \frac{\alpha_y^\chi \alpha_z^\chi}{c^2}, \quad (\text{C20})$$

which is the result quoted in Eqs. (22) and (23) of the main text. The current j_{3D} introduced therein is the sum of the right hand side of Eq. (C20) over the valleys.

Figures 4 and 5 display $j_{2,x}(z) = \sum_\chi j_{2,x}^\chi(z)$ and $\overline{j_{2,x}} = \sum_\chi \overline{j_{2,x}^\chi}$, respectively, for the case in which the two valleys are related by a mirror plane perpendicular to the z -axis ($\alpha_y^\chi = \alpha_y$ independent of χ and $\alpha_z^\chi = \chi \alpha_z$).

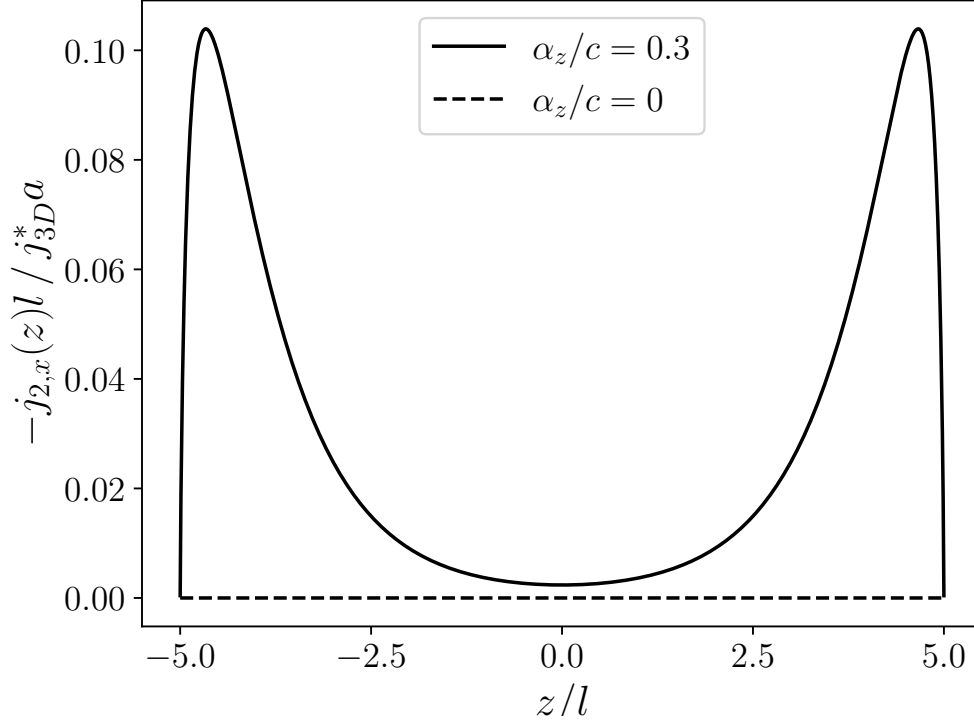


FIG. 4. Spatially resolved nonlinear current density for $\bar{a} = 10$ and $\bar{\alpha}_y = 0.3$. A tilt-independent normalization current $j_{3D}^* = j_{3D}/(\bar{\alpha}_z \bar{\alpha}_y)$ is defined, $j_{3D}^* a$ being independent of a . We see that $j_{2,x}(z)$ is even in z .

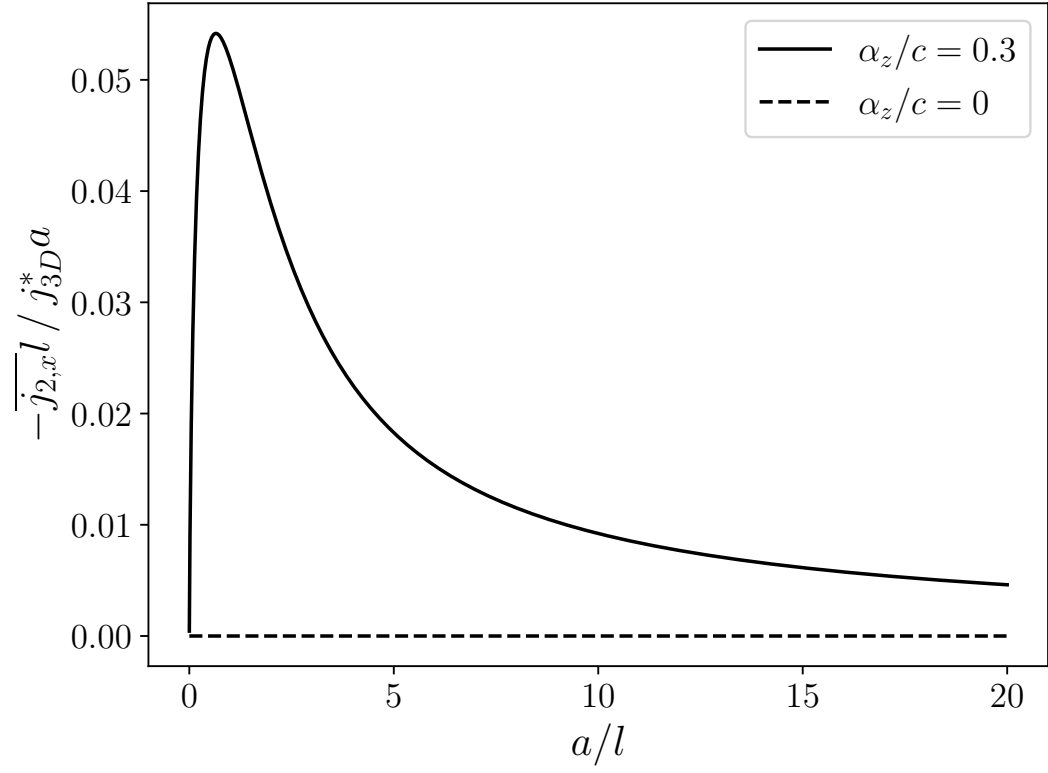


FIG. 5. Average current as a function of the film thickness for $\tilde{\alpha}_y = 0.3$. We observe $\overline{j_{2,x}} \rightarrow 0$ when $\tilde{a} \rightarrow \infty$ and $\tilde{a} \rightarrow 0$, with a maximum occurring for $\tilde{a} \approx 0.5$.